UDC 621.314 https://doi.org/10.20998/2074-272X.2023.6.07

O.I. Khrysto

Current-voltage characteristics of single-stage semiconductor magnetic pulse generators with a distinctive structure of the conversion link in the input circuit

Introduction. *The main feature of the semiconductor magnetic pulse generators (SMPGs) is a slow accumulation of energy in the primary capacitor and its rapid introduction into the load by using a series of sequentially connected magnetic compression stages. Initially, these devices were mainly used for pumping gas lasers, but over the last decade SMPGs have been increasingly used in electric discharge technologies for water purification and air ionization to remove toxic impurities. At the same time, along with the practice of using these devices, development has also been achieved in the principles of their design and methods of mathematical modeling.* ***Problem***. *The main drawback of the existing theory of SMPG's stationary oscillations mode is an adoption of the saturable reactor (SR) model in approximation of the static magnetization curve of its core, as well as unidirectional nature of the energy transfer from the generator to the load. In most publication the exchange processes between the power source and SR are still not covered.* ***Goal***. *Study of electrical and energy characteristics of low-voltage single-stage SMPG devices with series and parallel conversion stages in the charging circuit.* ***Methodology***. *To achieve the set goal, this work uses comprehensive approach relayed on technical tools of setting up the experiment, numerical methods for processing measurement results, as well as an analytical method for describing electromagnetic processes in single-stage SMPG circuits.* ***Results***. *The closed current-voltage characteristics of the SR are obtained, according to which the numerical calculations of the integral magnetic and energy characteristics of the proposed models are carried out. The features of the longitudinal capacitance charging process in a SMPG's circuit with a parallel conversion stage, which occurs simultaneously in two adjacent circuits, are explained. Analytical expressions to describe the dynamics of magnetic flux density in the SR's core as a time-depended function are derived. Based on the obtained hysteresis curve of the core, the exchange processes of energy transfer between the power source and the SR are explained.* ***Practical value***. *The results of the research can be applied in the development of low-voltage SMPG circuits with improved energy-dynamic parameters.* Reference 15, figures 8.

Key words: **semiconductor magnetic pulse generator, commutating choke, conversion link, electrical and energy characteristics, displacement current, energy losses dynamics.**

У роботі проведено експериментальне дослідження одноступеневих магнітно-напівпровідникових генераторів імпульсів з відмітною структурою зарядно-розрядного перетворювача у вхідному контурі. Наведено електричні параметри кожної схеми, відмічено фізичні й конструктивні особливості комутуючого дроселя вихідної ланки компресії імпульсів, та описано технічні засоби проведення експерименту. Отримано замкнуті вольт-амперні характеристики комутуючого дроселя, відповідно до яких проведено числові розрахунки інтегральних магнітних та енергетичних характеристик запропонованих моделей. Виведено аналітичні вирази для опису динаміки магнітної індукції в осерді дроселя за часом. На основі кривої гістерезису осердя роз'яснено обмінні процеси передачі енергії між джерелом живлення та комутуючим дроселем. Розглянуто енергетичні характеристики магнітно-напівпровідникових генераторів імпульсів в залежності від струму підмагнічування. Пояснено особливості заряду повздовжньої ємності у схемі з паралельною перетворювальною ланкою, що відбувається одночасно у двох суміжних колах. Отримано залежності споживаної потужності від напруги джерела живлення та виконано аналіз цих характеристик за різним співвідношенням між повздовжньою та поперечною ємністю суміжних ланок компресії імпульсів. Результати досліджень можуть бути застосовані при розробці низьковольтних магнітно-напівпровідникових генераторів імпульсів з поліпшеними енергодинамічними параметрами. Бібл. 15, рис. 8.

Ключові слова: **магнітно-напівпровідниковий генератор імпульсів, комутуючий дросель, перетворювальна ланка, електричні та енергетичні характеристики, зсувний струм, динаміка втрат енергії.**

Problem definition. The research presented is a continuation of the author's previous cycle of works on this topic [1, 2], which highlights the principles of construction, physical and mathematical modelling of semiconductor magnetic pulse generators (SMPGs), both high and low voltage, with the aim of finding more rational circuit solutions, special modes of their operation and methods of efficient energy transfer from the generator to the load.

Analysis of recent research and publications. SMPGs belong to the class of converting technology devices that serve to amplify the peak power of the pulse on the load [3, 4]. They are widely used in a number of electric discharge technologies, where it is necessary to have powerful current pulses of submicrosecond duration with a sharp leading edge, for example, for powering microwave devices or pumping gas lasers on metal vapors [5, 6]. In recent years, the relevance of using these devices has increased significantly with the need for air purification from sulfur dioxide [7, 8] and wastewater disinfection [9, 10]. The steady-state mode of electromagnetic oscillations in SMPGs is mainly achieved under the condition of amplitude asymmetry between the main and return pulses, while the energy transfer processes between pulse compression links are usually considered assuming their unidirectionality from the generator to the load [11]. Mathematical modelling allows the application of approximation by the magnetization curve of the commutating choke (saturable reactor, SR), however, it still remains «static» [12, 13], i.e. in approximation to the slow process of magnetization of its core, and allows to obtain only an indirect judgment about the characteristics of the magnetic flux density and the dynamics of losses energy for remagnetization in the SR core. As is known from [14], the conversion link of the charging circuit and the first link of pulse compression determine the mode of operation of the generator, while the role of the following magnetic compression elements is to bring the pulse to a certain duration. Therefore, in the current work, attention is focused on the experimental

study of single-stage SMPGs, which differ in the conversion link in the input circuit. Moreover, in contrast to previous mathematical models of various variants of SMPG, these studies are defined as experimental, as superior in terms of their availability and effectiveness.

Separation of the previously unsolved part of the tasks. Despite the large number of publications on this topic, the processes of energy exchange between the power source and the SR, which noticeably increase with the increase of the displacement currents caused by the asymmetric mode of electromagnetic oscillations in various SMPG circuits, have remained aside.

The goal of the work is to study the electrical and energy characteristics of single-stage SMPGs with a distinctive converting link (serial or parallel) of electricity in the input circuit.

Research methods. Physical modelling of electromagnetic processes using appropriate technical means; numerical and analytical modelling; data processing by means of Excel.

Main material. In the work, an analysis of low-voltage (up to 1 kV output voltage) SMPGs with a series pulse compression link on the load, which differ in the structure of the charge-discharge converter in the input circuit and the method of restoring the magnetic flux density in the core of the SR to the initial state, is carried out. Based on the theoretical models of high-voltage SMPGs, considered in the previous work of the author [15], the basis of this study was precisely various options for the construction of the input converter of electricity, separating the part of the device that contains the voltage increase link (high-voltage transformer). These converters can be conventionally divided into one- and two-key, containing a series, parallel, or series-parallel link in the input circuit of the SMPG. The main advantage of a parallel energy conversion link over a serial one is that in order to achieve remagnetization of the SR, it is not necessary to use an additional source of energy that generates a magnetizing current in its main winding, but on the contrary, the process of forming a reverse pulse occurs at the expense of the energy of the main power supply.

The circuit of the first version of the SMPG, which contains a series conversion link C_0-VT_0-VD_0-L_0 in the charging circuit and an additional source of displacement current E_b is shown in Fig. 1.

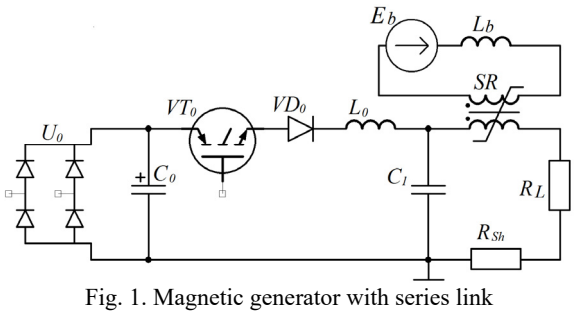

Fig. 1. Magnetic generator with series link in the charging circuit

The input of the device also contains a diode rectifier U_0 and a battery of capacitors C_0 with total capacity of 1 mF. Mains voltage to the diode rectifier is supplied through a step-down autotransformer, which allows for smooth adjustment of the input DC voltage. The charging choke L_0 must provide constant inductance, so it is designed on a ring magnetic core made of sprayed iron. The circuit was calculated based on the maximum accumulated energy stored in C_1, the duration of the input pulse and the compression ratio of the SR. For the parameters of the charging circuit of 32 μH and 1 μF, the duration of the current in this link is 10 μs. As the core of the SR, a ribbon magnetic core made of cobalt alloy (overall dimensions 50×34×30 mm) was used, which has high coefficient of rectangularity of the magnetic hysteresis loop. Taking into account the volume of the magnetic core – V_m = $3.2 \cdot 10^{-5}$ m^3, the range of the magnetic flux density – ΔB = 0.8 T, and the relative magnetic permeability in its saturated state – μ_S = 5, the compression ratio of the output link was x_k = 3.4 The generator was loaded with linear resistance R_L = 12 Ω, consisting of two parallel-connected low-inductance resistors, with total power of 120 W. The power supply sets the displacement current in the additional winding of the SR, which is connected through the decoupling choke L_b, which is designed to eliminate the variable component of the secondary winding of the SR. The inductance of the decoupling choke is 10 mH. The displacement current I_{bc} was set constant at the level of 1.5 A to ensure fast enough remagnetization of the SR.

A bifilar R_{Sh} current shunt with resistance of 0.16 Ω and a 1:10 voltage divider of a mixed type (resistive-capacitive) were used to measure the current-voltage characteristics of the SR. All measurements were made relative to the negative bus of the device, so the current shunt was located in the cut between C_1 and R_L. As indicated in Fig. 1, according to this variant of the SR placement, to measure the voltage on it, it is necessary to have a voltage difference between C_1 and R_L, but this complicates the calculation process due to the need for exact synchronization of three signals at once (SR current, voltage on R_L, voltage on C_1). If we place the SR in series near the shunt on the negative bus, then the voltage on its winding will be determined by subtracting the voltage drop on the shunt itself, which will facilitate further numerical calculations. Current signals on the shunt U_{Sh} and voltage on the SR U_{SR} are supplied through coaxial lines to the inputs of a two-channel memory oscilloscope SDS1022, which has a common negative terminal between its channels. Digitized data were stored in text format and transferred to Excel for mathematical calculations. The number of sampling points provided by the oscilloscope on each channel is 10^3 with interval of 40 ns and amplitude value in millivolts. Since the signals have an asymmetric shape, for their correct output on the oscilloscope screen, it is necessary to ensure the deviation of the position of the rays of these signals from the zero position, so the digitization results were transformed taking into account the vertical shift on each channel of the oscilloscope and the transmission coefficient on each signal according to the appropriate formulas:

$$U_c = (U_i - U_b)/100, \quad (1)$$

$$I_c = (I_i - I_b)/160, \quad (2)$$

where U_i, I_i are the discretized values of the voltage and

current signals of the SR; U_b, I_b are shifts to compensate for the deviation in mV; U_c, I_c are the normalized values of the voltage and current of the SR.

Below are the main formulas for calculation (analysis) of one-stage SMPG, which are applied in the Excel program.

Formulas for calculating SR with toroidal core:

Cross section of the core:

$$S_c = h \cdot (D - d)/2 , \tag{3}$$

where D, d, h are, respectively, the outer and inner diameters and height of the core.

The length of the middle line:

$$\ell_c = \pi \cdot (D + d)/2 . \tag{4}$$

The magnetic field strength:

$$H = (w \cdot I_c)/\ell_c , \tag{5}$$

where I_C is the current through the choke winding, w is the number of its turns.

The inductance of the choke with a uniformly distributed winding on the core:

$$L_{SR} = \mu_r \mu_0 \frac{w^2 \cdot S_c}{\ell_c} . \tag{6}$$

The magnetic flux density is proportional to the integral of the voltage on its winding and is defined as:

$$B = B_0 + \frac{1}{w \cdot S_c} \int U_c \mathrm{d}t , \tag{7}$$

where U_c is the voltage on the choke winding, B_0 is the initial magnetic flux density in the SR core.

The energy of the external power source spent on remagnetization of the core can be determined by the following equivalent expressions:

$$E_m = \int_0^{\tau} U_c \cdot I_c \cdot \mathrm{d}t = V_m \cdot \int_{-B}^{+B} \mathrm{d}B \cdot H , \tag{8}$$

where τ is the time at which a complete cycle of the passage of the hysteresis curve $B(H)$ occurs; V_m is the volume of the magnetic core of the SR.

For the integrals in the specified expressions, it is possible to approximate using the trapezoidal approximation method:

$$E_m = \frac{V_m}{2} \sum_{k=0}^{k=n} \left(H^{k+1} + H^k\right) \cdot \left(B^{k+1} + B^k\right), \tag{9}$$

where H^k, B^k are the discrete values of the magnetic field strength and the magnetic flux density in the core of the SR.

On the basis of the converted current and voltage signals of the SR, closed current-voltage characteristics were constructed for three values of the input voltage (U_{in} =120, 150, 180 V), which are shown in Fig. 2,*a*. A common feature of the obtained curves is their positive shift relative to the current axis and the same contour of the negative loop of the 3rd quadrant, which reproduces the process of forming the reverse polarity pulse. A distinctive feature is the growing contour of the hysteresis loops located in the 1st quadrant. The integral calculation of these curves takes place according to the time arrow starting from the zero position of the coordinate system. The area of each curve is proportional to the energy consumed by the power source, therefore, it can be argued that the difference between the areas of the 1st and 3rd quadrants will be directly proportional to the energy dissipated on the SR. The dependence of the magnetic flux density on the magnetic field strength and the dynamics of energy losses in the SR core was calculated according to the formulas indicated above, and the results are shown in Fig. 2,*b*. According to the obtained graphs, it is possible to note the tendency of the gradual expansion of the hysteresis area of the SR core with an increase in the input voltage, which is associated with an increase in the charge rate of C_1.

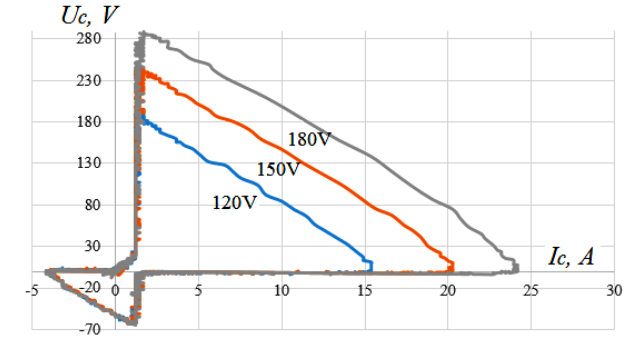

a

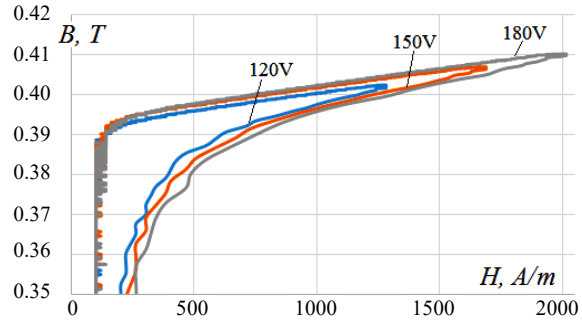

b

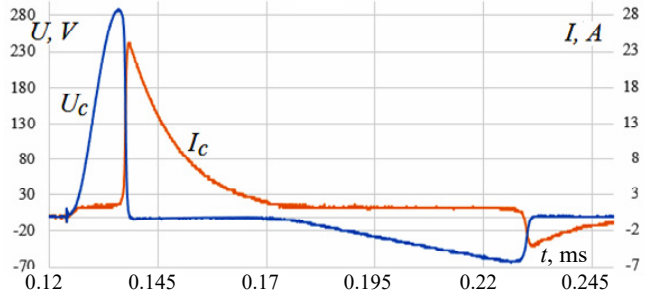

c

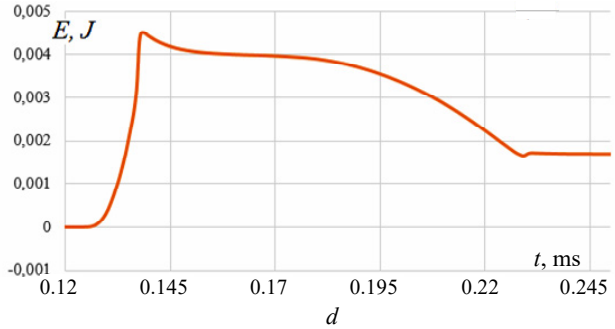

d

Fig. 2. Electromagnetic characteristics of the SR: *a*) current-voltage characteristics; *b*) magnetic flux density in the core; *c*) voltage and current oscillograms; *d*) dynamics of remagnetization energy

The maximum amplitude of the charge of the capacity C_1 from the capacity of the power source C_0 is determined according to the derived expression:

$$U_{\max}(t_1) = U_{C1} + \frac{U_{c0} - U_{c1}}{L_0 \cdot \omega_1 \cdot C_1} \cdot \left(\frac{\omega_1}{\alpha_1^2 + \omega_1^2} \cdot \exp(\alpha_1 \cdot t_1) \right), \quad (10)$$

where the cyclic frequency of oscillations of the charging circuit ω_1, the duration of its half-wave t_1 and the attenuation decrement α are determined respectively as

$$\omega_1 = \frac{\sqrt{\left| R_0^2 \cdot C_0^2 \cdot C_1^2 - 4 \cdot L_0 \cdot C_0 \cdot C_1 \cdot (C_0 + C_1) \right|}}{2 \cdot L_0 \cdot C_0 \cdot C_1}; \quad (11)$$

$$t_1 = \pi / \omega; \quad \alpha = -R_0 / 2 \cdot L_0 .$$

If we assume that the current through the SR on the main magnetization curve has a sufficiently small value compared to the current in its saturation, then the law of change of magnetic flux density in its core will be determined by the voltage on the capacitor C1 and can be written as:

$$B(t) = -B_s + \frac{1}{S_m \cdot w_1} \cdot \left(\begin{array}{l} U_{C0} \cdot t + \\ + \dfrac{U_{c1} - U_{c0}}{L_0 \cdot \omega_1 \cdot C_1} \cdot \dfrac{\omega_1^2}{\left(\alpha_1^2 + \omega_1^2\right)^2} \times \\ \times \exp(\alpha_1 \cdot t) \cdot \sin(\omega_1 \cdot t) \end{array} \right). \quad (12)$$

The process of returning the magnetic flux density to the initial state occurs due to the action of the magnetization current I_{bc} from the source E_b in its additional winding w_2, which accordingly transforms the displacement current into the main winding w_1 equal to:

$$i_b = -I_{bc} \cdot w_1 / w_2 . \quad (13)$$

This current will create linearly increasing voltage on C_1 of reverse polarity before the appearance of an operating pulse, which is described by a linear law:

$$U_{C1} = -\frac{I_{bc} \cdot w_1}{C_1 \cdot w_2} t . \quad (14)$$

Integrating this equation over time in accordance with (7), we obtain the expression for the magnetic flux density on the reverse remagnetization interval:

$$B(t) = B_s - \frac{I_{bc} \cdot w_1}{2 \cdot S_c \cdot w_1 \cdot C_1 \cdot w_2} t^2 , \quad (15)$$

where B_s is the magnetic flux density of the SR core saturation.

That is, in the reverse process, the magnetic flux density will change according to the parabolic law, and its full dynamics is shown in Fig. 3,*b*.

As noted in Fig. 3,*a*, the hysteresis loop has a positive shift along the axis of the magnetic field strength due to the magnetization current, which affects the energy interaction between the power source and the SR core, which stores the energy of the magnetic field. According to the obtained graph of energy losses due to remagnetization of the core (Fig. 2,*d*), the hysteresis curve can be divided into sections where the work of the external power source has both positive and negative values. In the field section from residual magnetic flux density to positive saturation magnetic flux density (curve 1–2 in Fig. 3,*a*), the work of the external power source (energy of capacitor C_1) is performed due to magnetization of the core, with dB>0 and H>0, so the resulting energy gain according to (9) dE_m>0. At the moment of saturation of the SR and the introduction of energy into the R_L load, a slight its increase is observed in the graph of the dynamics of energy loss (Fig. 2,*d*). But already at the stage of formation of the reverse voltage, a significant part of the energy accumulated in the core of the SR will return to the power source (curve 2–3 in Fig. 3,*a*), because in this section the fields dB<0 and H>0, and the resulting increase in energy losses, respectively, is dE_m<0. At the moment of reaching the magnetic flux density of the opposite value $-B_s$, the work of the power source will also be positive (dB<0, H<0), because the magnetic field strength becomes negative, which is noted on the curve (Fig. 2,*d*) by its slight increase (curve 3–4), but this increase will be compensated at the stage of formation of a new operating pulse (curve 4–3).

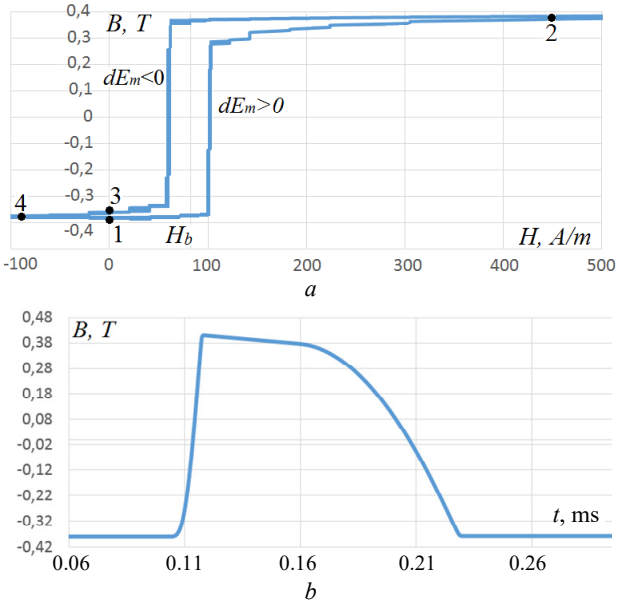

Fig. 3. *a* – magnetic hysteresis loop with shift by H; *b* – dynamics of magnetic flux density B over time

The principle of operation of the SMPG circuit in the absence of magnetization current differs in that the amplitude of the output pulse decreases, but at the same time the power consumption increases depending on the input rectified voltage on the C_0 capacitor, which is shown in Fig. 4. In this mode, the SR operates by a partial magnetization curve, therefore the working drop of the magnetic flux density in the core is reduced and, accordingly, the delay in its saturation, which gradually disappears completely, and the characteristic of the peak pulse voltage reaches its saturation. Since there is no time delay between the closing of the transistor VT_0 and the saturation of the SR, the discharge current will be closed not only along the C_1–SR–R_L circuit but also along the C_0–VT_0–SR–R_L circuit, which will additionally increase the energy of the pulse at its amplitude even lower for the input one.

The following SMPG circuit is already based on a parallel conversion element and a charging choke in the input circuit. This version of the device allows to avoid the use of an additional source of displacement current, but with the difference from the previous version of the SMPG that it generates pulses of inverse polarity on the load. In the circuit (Fig. 5), the mains alternating voltage

from the autotransformer, the diode rectifier and the electrolytic capacitor are combined into one element and represented by a constant voltage source E_0.

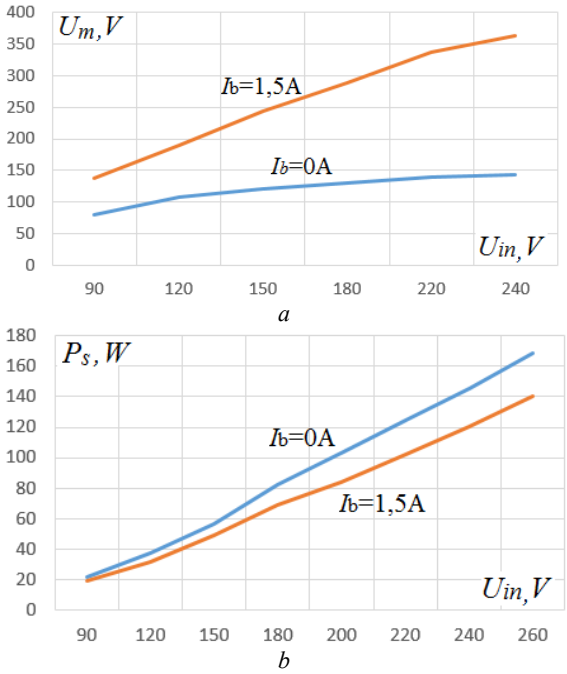

Fig. 4. Characteristics of the amplitude value of the pulse voltage U_m on the load (*a*) and the power consumption of the device P_s (*b*) depending on the constant input voltage U_{in} on C_0

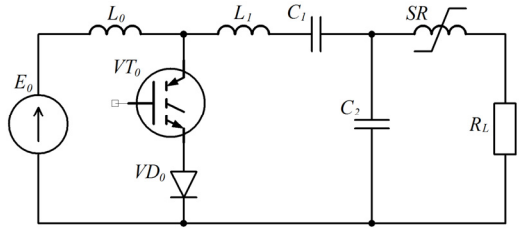

Fig. 5. SMPG circuit with parallel conversion link in the input circuit

A distinctive feature of the SR circuit with parallel conversion link is that its closed current-voltage characteristics (Fig. 6) become directly opposite to the characteristics of the first version of the SMPG, namely, the working and return pulses are described in the 3rd quadrant and the 1st quadrant of the system coordinates, respectively. The characteristics have a negative current shift, but unlike the previous SMPG model, this shift turns out to be dependent on the input voltage of the power supply E_0.

When approaching the ideal model of the SR, the charge-discharge processes in the circuit can be considered separately and divided into several intervals along separate circuits. When VT_0 is unlocked in the circuit C_1–L_1–VT_0–C_2, the discharge process of C_1 to C_2 begins with partial energy transfer, due to the presence of charging current from the power source, therefore, after locking VT_1, there will be residual voltage on C_1. This process is shown in Fig. 7,*a*, where the voltage on the capacitor C_1 is obtained as a result of the calculation, as the difference between the numerical data of the voltages on VT_0 and C_2.

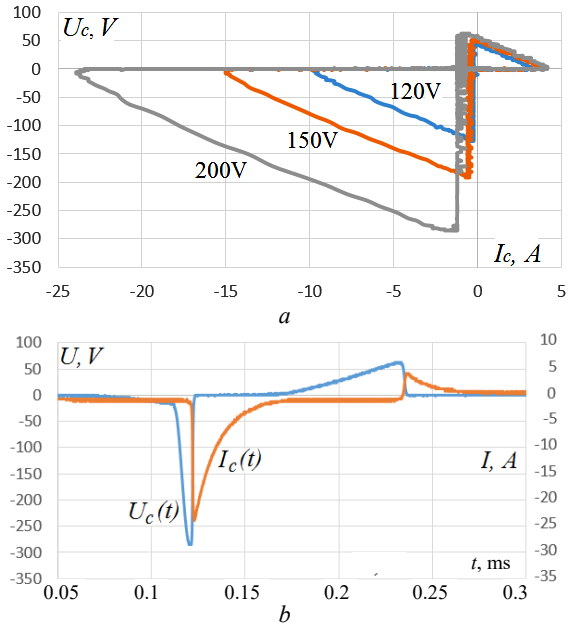

Fig. 6. Electrical characteristics of the SR: *a* – closed current-voltage characteristics; *b* – oscillograms of voltage and current

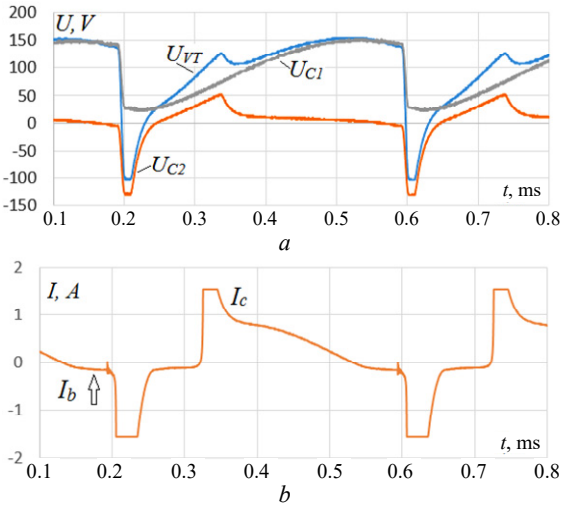

Fig. 7. *a* – voltage characteristics on capacitors; *b* – characteristic of the current through the SR

After blocking VT_0, the charging phase of series-connected C_1 and C_2 in the circuit E_0–L_0–L_1–C_1–C_2 begins. Due to the relatively low natural frequency of oscillations of this circuit, the voltage on C_2 increases almost linearly. At the same time, the magnetic flux density in the core of the SR changes its value to the opposite, and when saturation magnetic flux density is reached, C_2 energy is reset to the load. At this stage, the charging current will be closed to the load through the inductance of the saturated SR winding within the circuit E_0–L_0–L_1–C_1–SR–R_L. Here, the capacity C_1 continues to charge according to the oscillating law to its maximum value, and the voltage on C_2 will remain at the residual level due to its shunting to the load by the SR winding. The current in the SR winding as shown in Fig. 7,*b*, also displays part of the charge current of capacitor C_1. When the voltage on C_1 reaches its maximum value, the current through the SR changes its direction and relatively small displacement biasing current I_b is formed, which, as it turns out, depends on the voltage of the power source.

At this stage, the SR core leaves the state of reverse saturation and, in the process of charging C_2, is magnetized along the main curve to the opposite saturation limit. Since the C_1 charge process occurs simultaneously in two circuits, for the analytical determination of the displacement current through the SR winding, it is necessary to solve the characteristic equation of the 4th order and find the unknown coefficients of the harmonic equations, which complicates the calculation process enough. Considering the fact that the inductance of the outer circuit consists of L_0 and the inductance of the SR in its unsaturated state, when the relative permeability of its core is sufficiently large ($\mu = 10^5$), its oscillation frequency will be lower than the frequency of the inner circuit. In addition, the initial voltage difference between C_0 and C_1 will be higher for the inner circuit, so the displacement current through the SR will be a smaller part of the charging current of C_1. Therefore, it can be assumed that the displacement current of the external circuit will modulate the charging current of C_1 until the moment of saturation of the SR from the linearly increasing voltage on C_2. Thus, the oscillatory processes in the considered circuits can be described by similar analytical expressions specified above, taking into account the parameters of each circuit. For example, for the above charging circuit with E_0–L_0–L_1–C_1–SR–R_L, its cyclic frequency ω_2 and attenuation decrement α_2 can be found by the formulas:

$$\omega_2 = \frac{\sqrt{\left|\begin{array}{l} R_L^2 \cdot C_0^2 \cdot C_1^2 \cdot C_2^2 - 4 \cdot (L_0 + L_1 + L_{SR}) \times \\ \times C_0 \cdot C_1 \cdot C_2 \cdot (C_0 \cdot C_1 + C_1 \cdot C_2 + C_0 \cdot C_2) \end{array}\right|}}{2 \cdot (L_0 + L_1 + L_{SR}) \cdot C_0 \cdot C_1 \cdot C_2}; \quad (16)$$

$$\alpha_2 = -\frac{R_L}{2 \cdot (L_0 + L_1 + L_{SR})}.$$

The maximum voltage on each capacitor is determined according to (10), but taking into account the algebraic sum of the initial values of the voltages on the three capacitors U_{C0}–U_{C1}–U_{C2} and the sum of the inductances L_0+L_1+L_{SR} of this circuit. The value of the displacement current through the SR is approximately determined as:

$$i_b(t) = \frac{U_{C0} - U_{C1}}{(L_0 + L_{SR}) \cdot \omega_2} \sin(\omega_2 \cdot t) \cdot \exp(\alpha_2 \cdot t), \quad (17)$$

where the inductance L_{SR} is determined by the formula, as for the toroidal core (6). It was determined that the initial voltage U_{C1} on the capacitor C_1 is the maximum voltage when the core is magnetized L_{SR}.

It was established that due to the fact that the C_1 charge occurs according to the oscillatory law, the dependence of the output pulse amplitude on the switching frequency of the transistor is observed. In the frequency range from 1.2 to 1.8 kHz, the amplitude of the main pulse is significantly weakened, which is accompanied by a decrease in power consumption. By the time of the new switching of VT_0 due to the oscillating charge of C_1, the capacity C_2 has time to recharge again and therefore another pair of pulses of the main and reverse polarity is formed. It was found that if the switching region of VT_0 coincides with the moment of formation of the demagnetization pulse, then the charging current of C_2 will be shunted by the inductance of the saturated SR, which causes a significant decrease in the working pulse. In another case, when the moment of switching coincides or occurs before the moment of recharging C_2, the amplitude of the pulse on it only increases. According to this study, it was established that for the correct operation of the device, the generation frequency should be at least 2-2.5 kHz.

The dependencies of the power consumption characteristics and the output pulse amplitude on the input voltage of the power source at the generation frequency of 2.5 kHz for 3 values of the transverse capacitance C_2 and the fixed capacitance C_1 = 1 μF are shown in Fig. 8.

The obtained graphs can be analyzed as follows, namely: an increase in the capacity C_2 from 0.5 to 1.5 μF leads to a deeper discharge of the capacitor C_1, therefore the charging voltage drop on it becomes more significant, which causes an increase in the charging current and power consumption of the SMPG. When C_1<C_2, the pulses on the load become longer and are characterized by a decrease in their amplitude (Fig. 8,*b*). On the contrary, for C_1>C_2, the capacity C_1 is no longer completely discharged, therefore, a significant residual voltage is formed on it, which reduces the jump in the charging current. It can be noted that the power characteristic grows according to quadratic laws and corresponds to the energy accumulated in C_1 at the time of switching VT_0. Calculations also showed that the dependencies of energy losses in the core on the input supply voltage are characterized by the presence of their threshold value, after which the energy losses stop increasing, which can occur in the case of the hysteresis loop of the SR core reaching its maximum expansion. The maximum energy losses in the SR core during one magnetization cycle for this SMPG circuit at input voltage of 280 V do not exceed 1.5 mJ. The considered circuit solutions of low-voltage semiconductor magnetic pulse generators are expedient to be used in modern advanced electroimpulse material processing technologies.

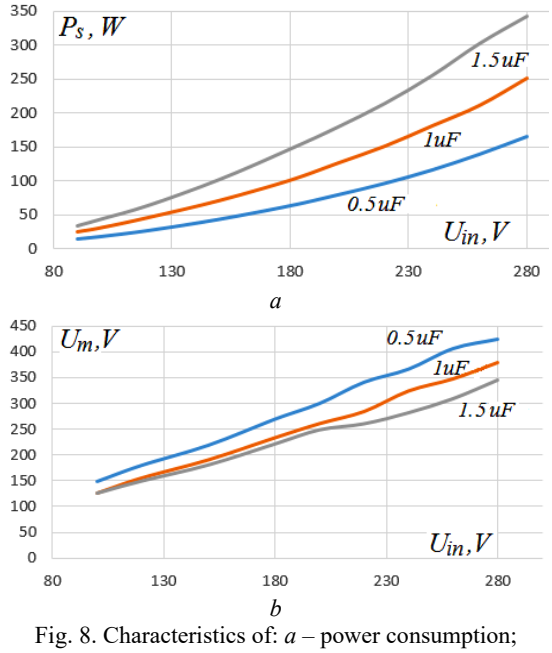

Fig. 8. Characteristics of: *a* – power consumption; *b* – output pulse amplitude for 3 values of capacitance C_2

Conclusions.

1. According to the numerical analysis performed on the experimental current-voltage characteristics of the single-stage SMPG circuit with a series conversion link in the input circuit, it was determined that a significant part of the energy at the stage of the remagnetization process of the SR core is returned to the power source. In contrast to the symmetrical hysteresis loop, which is characteristic of two-stroke circuits of magnetic pulse generators without external biasing, the presence of a significant fraction of negative energy in the magnetization characteristic of the SR is caused by the presence of constant displacement current through its winding, which increases the area of the magnetic field where its flux density and strength have opposite values.

2. On the basis of the experimentally obtained closed current-voltage characteristics of the commutating choke for the SMPG circuit with a parallel conversion link in the input circuit, the presence of displacement current, the value of which depends on the input supply voltage, was established for the first time. Based on the considered oscillatory processes in adjacent charging circuits, an analytical equation is proposed for estimating the displacement current, which plays an important role at the stage of energy return from the commutating choke to the power source.

3. It is established that the power consumption of the SMPG with a parallel conversion link in the input circuit depends on the ratio of capacities in the adjacent pulse compression links. A decrease in the residual voltage on the longitudinal capacitance leads to an increase in the charging current and power consumption. When the condition $C_1>C_2$ is met, the generator generates pulses with larger amplitude and shorter duration on the load.

Acknowledgments. The author expresses sincere gratitude to Dr. V.I. Zozulev for his unique understanding of practical ways of improving power converters of electricity and valuable recommendations provided during the discussion of the results of this work.

Conflict of interest. The author declares no conflict of interest.

REFERENCES

1. Khrysto O. Energy transfer processes in high-voltage circuits based on magnetic pulse compression. *Acta Electrotechnica et Informatica*, 2020, vol. 20, no. 3, pp. 3-10. doi: https://doi.org/10.15546/aeei-2020-0013.

2. Volkov I.V., Zozulev V.I., Khrysto O.I. Increasing of the efficiency of power electronics devices by the control of charging time of the capacitors in their circuits. *Technical Electrodynamics*, 2019, no. 2, pp. 15-18. (Ukr). doi: https://doi.org/10.15407/techned2019.02.015.

3. Golubev V.V., Zozulov V.I., Marunia Yu.V., Storozhuk A.I. Development of principles of construction and improvement of magnetic-semiconductor pulse devices of power converter technology. *Proceedings of the Institute of Electrodynamics of the National Academy of Sciences of Ukraine*, 2022, no. 62, pp. 34-40. (Ukr). doi: https://doi.org/10.15407/publishing2022.62.034.

4. Li S., Gao J., Yang H., Zhu D., Qian B., Cui Y., Wu Q., Zhang J. Investigation on Adjustable Magnetic Pulse Compressor in Power Supply System. *IEEE Transactions on Power Electronics*, 2019, vol. 34, no. 2, pp. 1540-1547. doi: https://doi.org/10.1109/TPEL.2018.2830106.

5. Boyko N.I. Powerful generators of high-voltage pulses with nanosecond fronts. *Electrical Engineering & Electromechanics*, 2018, no. 1, pp. 59-61. doi: https://doi.org/10.20998/2074-272X.2018.1.09.

6. Ghodke D.V., Muralikrishnan K., Singh B. New multiplexed all solid state pulser for high power wide aperture kinetically enhanced copper vapor laser. *Review of Scientific Instruments*, 2013, vol. 84, no. 11, art. no. 113102. doi: https://doi.org/10.1063/1.4829075.

7. Bozhko I.V., Zozulev V.I., Kobylchak V.V. SOS-generator for the electric discharge technology used pulse barrier discharge. *Technical Electrodynamics*, 2016, no. 2, pp. 63-67. (Ukr). doi: https://doi.org/10.15407/techned2016.02.063.

8. Pokryvailo A., Yankelevich Y., Wolf M. A High-Power Pulsed Corona Source for Pollution Control Applications. *IEEE Transactions on Plasma Science*, 2004, vol. 32, no. 5, pp. 2045-2054. doi: https://doi.org/10.1109/tps.2004.835952.

9. Guo X., Zheng D., Blaabjerg F. Power Electronic Pulse Generators for Water Treatment Application: A Review. *IEEE Transactions on Power Electronics*, 2020, vol. 35, no. 10, pp. 10285-10305. doi: https://doi.org/10.1109/TPEL.2020.2976145.

10. Akiyama H., Akiyama M. Pulsed Discharge Plasmas in Contact with Water and their Applications. *IEEJ Transactions on Electrical and Electronic Engineering*, 2021, vol. 16, no. 1, pp. 6-14. doi: https://doi.org/10.1002/tee.23282.

11. Balcerak M., Hołub M., Pałka R. High voltage pulse generation using magnetic pulse compression. *Archives of Electrical Engineering*, 2013, vol. 62, no. 3, pp. 463-472. doi: https://doi.org/10.2478/aee-2013-0037.

12. Choi J. Introduction of the magnetic pulse compressor (MPC) – fundamental review and practical application. *Journal of Electrical Engineering and Technology*, 2010, vol. 5, no. 3, pp. 484-492. doi: https://doi.org/10.5370/JEET.2010.5.3.484.

13. Nejadmalayeri A.H., Bali Lashak A., Bahrami H., Soltani I. A high voltage isolated pulse generator using magnetic pulse compression and resonant charging techniques for dielectric barrier discharge applications. *Journal of Electrical and Computer Engineering Innovations*, 2021, vol. 9, no. 2, pp. 239-248. doi: https://doi.org/10.22061/jecei.2021.7519.400.

14. Volkov I.V., Zozulov V.I., Golubev V.V., Paschenko V.V., Storozhuk A.I. Optimization of structural units of magnetic - semiconductor pulse generators. *Proceedings of the Institute of Electrodynamics of the National Academy of Sciences of Ukraine*, 2019, no. 53, pp. 65-74. (Ukr). doi: https://doi.org/10.15407/publishing2019.53.065.

15. Khrysto O.I. Electrical and energy characteristics of the serial-parallel converter unit of a high-voltage semiconductor - magnetic pulse generator. *The Bulletin of National Technical University «KhPI». Series: Techniques and Electrophysics of High Voltage*, 2015, no. 51, pp. 99-106. (Ukr).

Received 11.03.2023
Accepted 04.05.2023
Published 02.11.2023

O.I. Khrysto[1]*, PhD, Senior Researcher,*
[1] Institute of Pulse Processes and Technologies of NAS of Ukraine,
43-A, Bogoyavlenskij Avenue, Mykolayiv, 54018, Ukraine,
e-mail: alexander.khristo@gmail.com

How to cite this article:
Khrysto O.I. Current-voltage characteristics of single-stage semiconductor magnetic pulse generators with a distinctive structure of the conversion link in the input circuit. *Electrical Engineering & Electromechanics*, 2023, no. 6, pp. 41-47. doi: https://doi.org/10.20998/2074-272X.2023.6.07